IEEE Access
Multidisciplinary ⋮ Rapid Review ⋮ Open Access Journal

Received 7 December 2023, accepted 20 December 2023, date of publication 25 December 2023,
date of current version 29 December 2023.

Digital Object Identifier 10.1109/ACCESS.2023.3346681

RESEARCH ARTICLE

Unmanned Aerial System Trajectory Tracking Based on Diversified Grey Wolf Optimization Algorithm

PARUL PRIYA, (Member, IEEE), AND SUSHMA S. KAMLU
Department of Electrical and Electronics Engineering, Birla Institute of Technology, Mesra, Ranchi 835215, India
Corresponding author: Parul Priya (parulpriya.ee@gmail.com)

ABSTRACT Trajectory tracking is one of the most important aspects of an unmanned aerial system (or quad-copter) for selecting the optimal path from the source to the destination. This article presents a mathematical framework and approach for addressing the challenge of nonlinear systems like quad-copter. A novel control system for the quad-copter's positions (z, y, x) and attitudes (roll (ϕ), yaw (ψ), pitch (θ)) has been proposed based on optimisation techniques that are integrated with proportional-integral (PI) controllers. Astute position update methods such as helical, circular, etc. have been introduced using different algorithms like particle swarm optimization (PSO), grey Wolf optimization (GWO), and the diversified grey wolf optimizer (DGWOA) algorithm. Following that, in an iterative procedure, a variety of leadership levels are used to update the individual's position, and the leadership is modified through the use of an adaptive mechanism. For validation, the proposed algorithm's effectiveness is evaluated based on the convergence rate compared to that of other meta-heuristic algorithms. Owing to its inadequate exploration, PSO leads to challenges with parameter selection, whereas GWO is easy to get to the local optimum. The concept and execution of DGWOA have been implemented to update the Unmanned Aerial Systems (UAS) controlled parameters in order to overcome these limitations. The proposed algorithm's performance for path planning in a complex and cluttered environment is investigated. The simulation shows that the DGWOA algorithm has a faster response as compared to the reference and (z, y, x) has been improved with (92.87, 96.95, and 99.69) percentage along with eliminating the shortcomings of PSO & GWO.

INDEX TERMS Meta-heuristic algorithm, optimization techniques, PID controller, trajectory tracking, under actuated quadcopter.

I. INTRODUCTION

In many countries, research on unmanned flying technology is thriving [1], [2]. Unmanned Aerial Systems (UAS) have drawn increased attention as a type of contemporary aerial weaponry because of its capacity to operate in challenging and dangerous conditions [3] and easy and quick delivery of humanitarian supplies. For the efficient operation of UAS, flight path optimization is required for quick and easy movement of these aerial vehicles. The problem of designing a flight path could be viewed as a difficult optimization problem that needs to be solved by effective algorithms. The advancement of UASs technology depends on 3D flight route optimization technology.

Among the various controllers used by various researchers, LPID control is one of the most popular controllers. A nonlinear PI/PID controls the movements of UAS employing a nonlinear PID controller for horizontal movement and another for vertical movement and coordination. Nonlinear Control strategy takes into consideration acceleration and the velocity vector of a UAS featuring parameter tuning, which is constructed by making use of a genetic algorithm [4]. An adaptive controller with many models is created to reduce the impact of parametric uncertainties regarding the quadrotor system, specifically targeting the yaw and altitude channels [5]. Table 1 summarizes

The associate editor coordinating the review of this manuscript and approving it for publication was Diego Oliva.

a study of the existing control methods described in the literature.

Numerous uncertainties, such as shifting loads, outside disturbances, and shifting system parameters, are present and are difficult for traditional control systems to handle effectively. Conventional controllers must be combined with intelligent tuning strategies to balance the system's robustness and flexibility while controlling under actuated, multi-input, and strongly coupled UAS systems. Meta-heuristic algorithm-based path planning and control methodology studies have attracted attention.

The optimal path problem has grown to include the route that minimizes distance traveled, average altitude, fuel consumption, radar vulnerability, and other variables. Path optimization is a challenging task since it demands numerous search sources. Metaheuristic algorithms are intelligent algorithms that draw inspiration from nature [6], [7], which indicates that they were developed by imitating natural phenomena or the cooperative behaviours of creature(s). These optimization techniques can seek a collection of relevant attribute values and solve difficult optimization problems by minimizing or maximizing the objective function [8]. The route optimization problem has been solved using several meta-heuristic algorithms.

It has been proven that their ability to address nonlinear design problems with rapidity and precision. Additionally, it has rendered it possible to solve a wide range of difficult optimization problems. These applications include, for instance, those pertaining to layout optimization, signal processing, robot systems for scheduling problems, network distribution, route planning, power systems, fault detection, parameter optimization, system recognition, cluster analysis, mining data, computation of images, and transport problems [9]. To solve the purpose of a two-dimensional route optimization issue, the APSO approach having an adaptive weight factor premised on the PSO algorithm was introduced [10], avoiding the optimal local solution, the drawback of PSO. Merging the PSO method with optimum control [11], corrects the shortcomings of a single approach and improves surgical robot path planning. A new ACO-DE method for UASs 3D trajectory tracking was suggested in [12], enhancing the ant pheromone, updating procedure, and employing DE to optimize the pheromones of such an enhanced ACO model throughout the ant pheromone updating procedure. An enhanced cuckoo search method based on parallel and compact techniques was proposed, augmenting cuckoo search speed and accuracy while using less memory. The reallocation problem for heterogeneous UAVs with target position constraints has been solved using ACO and fuzzy C-means clustering [13] in detail.

Mirjalili et al. introduced the Grey Wolf Optimizer (GWO) technique as a meta-heuristic algorithm in 2014 [14]. This algorithm has excellent exploration abilities since it mimics the social organisation and hunting techniques of grey wolves. It is better than compared to certain other meta-heuristic algorithm(s) because of its flexibility, simplicity, and usability. A wide range of engineering specialties and control problems have been addressed with the GWO.

Reviewing the body of work that was presented in this paper and its findings revealed a several difficulties; the most frequent issues were minimal oscillations at the outputs and saturated stimuli over time caused by the jabbering phenomenon, non-optimal control systems, and instability in the presence of disturbances. These difficulties led to the development of an original concept to suggest a thorough and robust controlled framework that could function effectively for nonlinear systems agnostic of parametric as well as system modelling uncertainties. This work presents a unique NLPID controller with an incorporated meta-heuristic algorithm and PI Controller. A novel NLPID controller alters from the one introduced in the reference work [4]. The modification is achieved by optimizing all 6 coordinates of D-o-F i.e. ϕ, θ, ψ, x, y and z while considering the time factor, which was a constraint in the research work done earlier in this regard. Optimization of all these factors not only enhances the system's overall performance but augments the trajectory tracking of UAS as well. Systems with nonlinear dynamics that are affected by the different physical parameters require precise accuracy in trajectory tracking. Conventional controllers must be combined with intelligent tuning strategies to balance the system's robustness and flexibility while controlling under- actuated, multi-input, and strongly coupled UAS systems. In this context, the work has been designed for trajectory tracking based on the meta-heuristic algorithm. In this work, a modified GWO algorithm has been implemented to achieve the desired control parameters, and for the validation of the developed algorithm, it was further compared with other meta-heuristic algorithms for different case studies. Section VI discusses the result in detail, where the result has been compared with GWO and PSO, as only these depicted better candidates for comparison as others showed great variation in the result. A suggested multi-objective OPI, that represents the weighted combination of both the ITAE (Integral of Time Absolute Error) and the square value of the energy control is minimized by tweaking each of the twelve tuning parameters of the NLPID controller using a meta-heuristic algorithm.

The significant contributions of this study are summarized:

1) Thorough and robust controller framework capable of operating effectively for nonlinear systems regardless of parametric or system modeling uncertainties.
2) Using Hurwitz stability theorems, determine the stabilizing sets of a non-linear Conventional PI controller for a second-order unstable plant with delay time.
3) It has established a new strategy for dealing with constrained-based optimization problems that aims to solve complicated constrained concerns by incrementally constricting the scope of the search area until all constraints are met.
4) A novel non-linear stability concept based on the Diversified Grey Wolf Optimization (DGWOA) algorithm is

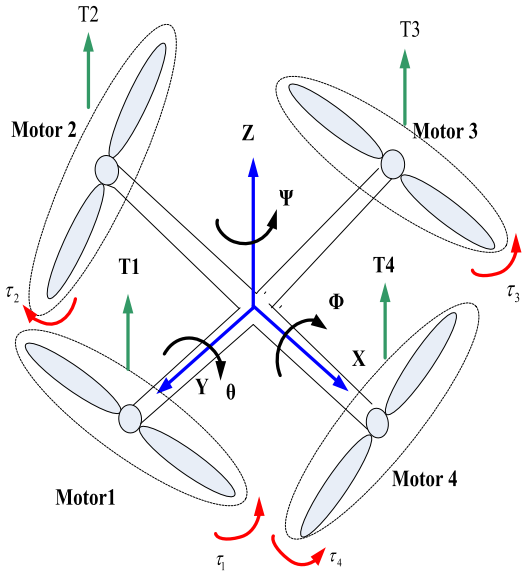

FIGURE 1. The movements and angles of quad-copter.

proposed, which is simple to implement, and simulation results show its efficacy and robustness.

The remainder of this essay is structured as follows. A brief review of the controls and dynamics of UAS is given in Section II. Estimating the controller parameter boundaries is covered in Section III. The proffered novel method of figuring out the stabilizing configurations of a NLPID controller is covered in full in Section IV, which also details the control and optimization strategies. The deployment of the optimization procedure for determining the ideal controller gains is described in Section V. Section VI presents the simulated and real-time results. A brief analysis of the findings, limitations, and future scope of the research is discussed in Section VII.

II. SYSTEM DESCRIPTION

As per the construction features, the UAS has been classified as fixed-wing and rotary-wing. The rotary-wing is further classified as a tri-copter, a quad-copter, and a hexa-copter and so on. This work is based on the quadcopter. The four propellers can be arranged in a cross or plus configuration that can be controlled independently. This makes it feasible to pivot in 6-degree-of-freedom (6-D-o-F), including three each of rotational and longitudinal degree-of-freedom. The UAS rotor speed can be altered to create lift force and movement. In this technique, the vertical movement is regulated by changing the speeds of all four propellers at the same instant. The speed of the 2nd and 4th propellers is modulated in inverse order to produce roll rotation and lateral movement. Pitch rotation and lateral motion are caused by controlling the speed of the 1st and 3rd propellers. The propeller movements and angles of UAS have been presented in Fig. 1.

A. KINEMATICS & DYNAMICS OF QUAD-COPTER

A fundamental model of system structure and disturbance dynamics is required for evaluating the performance and robustness of a system in the presence of uncertainty. Primarily, a mathematical framework must be derived to control any system. The mathematical structure will characterize the system's responses to various inputs. The inputs for the 6-D-o-F quad-copter system consist of combinations of the rotor speed $\left[\Omega_1\ \Omega_2\ \Omega_3\ \Omega_4\right]$ and the torques $\left[\tau_x\ \tau_y\ \tau_z\right]$, which in this case is a force f_t to control the altitude $[z]$ and to control the angles $\left[\phi\ \theta\ \psi\right]$ respectively. According to the model, the moments and forces generated by the rotors are related to the aircraft's position and attitude. Each parameter's significance is described in Table 2. Its dynamics can be formulated and characterized using two frames: a reference ground frame and a UASs frame. Both frames are linked by

TABLE 1. Review of related control techniques.

Sources	Implemented Technique(s)	Reason of Interest	Contribution of the paper
[15]	Mathematical formation of PID control	Uncertain Non-linear Systems	Introduced a mathematical model into the framework of the simple PI or PD (linear PID) control system for various classes(s) of MIMO non-linear unknown dynamic systems,
[16]	Dimensional control	Multi-quadrotor with suspended Load	Control the object's position and attitude, the yaw angle of the quadrotors, and the orientation of each cable.
[17]	Nonlinear parameter control	Quad-copter Slung Load.	Using the "input shaping" method, it can limit weight fluctuations during the movement.
[18]	PID Nonlinear	6-DOF quadrotor UAS	Optimize tracking while using less energy and fewer error than a PID linear controller.
[19]	Fractional order sliding modes	A load is grasped and transported by multi-quadrotors.	Grasping and transporting a load
[20]	PID	UAS	Define the acceptable limit for adjustment in moment of inertia and mass.
[21]	Quaternion based attitude controller	Quad-copter Slung Load	Keep providing minimum-load and high-amplitude change in oscillation for loads in unpredictable maneuvering.
[22]	LQR and Artificial intelligence	Quadrotor with suspended Load	Two take-off modes are investigated: without and with load.
[23]	Adaptive fault-tolerant control	Flexible cable-based Quad-copter Slung Load	Stabilize asymptotically while simultaneously adjusting the strict links to eliminate load fluctuations.

the following relations:

$$\upsilon = \Re \cdot \upsilon_B \tag{1}$$

$$\varpi = \Gamma \cdot \varpi_B \tag{2}$$

where $\upsilon = [\dot{x}\ \dot{y}\ \dot{z}]^T \in \mathbb{R}^3, \varpi = [\dot{\phi}\ \dot{\theta}\ \dot{\psi}]^T \in \mathbb{R}^3$, $\upsilon_B = [u\ v\ w]^T \in \mathbb{R}^3, \varpi_B = [p\ r\ q]^T \in \mathbb{R}^3$ and Γ is Angular transformation matrix and $\Re$ is rotation matrix, combination of inertial position co-ordinates and UASs reference co-ordinates.

The angular and linear velocity and/or position momemnts of the UASs is defined in (5), as shown at the bottom of the page. Table 2 depicts the dynamics of the UASs used in the subsequent (1)–(3), and (4), as shown at the bottom of the page.

$$\Gamma = \begin{bmatrix} 1 & Cn(\phi)Tn(\theta) & Sn(\phi)Tn(\theta) \\ 0 & -Sn(\phi) & Cn(\phi) \\ 0 & \dfrac{Cn(\phi)}{Cn(\theta)} & \dfrac{Sn(\phi)}{Cn(\theta)} \end{bmatrix} \tag{3}$$

The dynamic model of UASs in the inertial frame based on Euler-Newton formalization can be defined by means of (6) and (7), as shown at the bottom of the next page.

$$\left.\begin{aligned} \begin{bmatrix} \ddot{x} \\ \ddot{y} \\ \ddot{z} \end{bmatrix} &= g \begin{bmatrix} 0 \\ 0 \\ 1 \end{bmatrix} - \frac{ft}{m} \begin{bmatrix} Sn(\phi)Sn(\psi) + Cn(\phi)Cn(\psi)Sn(\theta) \\ Cn(\phi)Sn(\psi)Sn(\theta) - Cn(\psi)Sn(\phi) \\ Cn(\phi)Cn(\theta) \end{bmatrix} \\ \begin{bmatrix} \ddot{\phi} \\ \ddot{\theta} \\ \ddot{\psi} \end{bmatrix} &= \begin{bmatrix} 0 & \dfrac{Iy - Iz}{Ix}\dot{\psi} & 0 \\ 0 & 0 & \dfrac{Iz - Ix}{Iy}\dot{\phi} \\ \dfrac{Ix - Iy}{Iz}\dot{\theta} & 0 & 0 \end{bmatrix} \begin{bmatrix} \dot{\phi} \\ \dot{\theta} \\ \dot{\psi} \end{bmatrix} + \begin{bmatrix} \dfrac{\tau x}{Ix} \\ \dfrac{\tau y}{Iy} \\ \dfrac{\tau z}{Iz} \end{bmatrix} \end{aligned}\right\} \tag{6}$$

where total rotor thrust is a function of rotor thrust coefficient and square of rotor speed. Torque is a function of drag coefficient and rotor speed squared as given by (8).

$$\left.\begin{aligned} ft &= b(\Omega_1^2 + \Omega_2^2 + \Omega_3^2 + \Omega_4^2) \\ \tau x &= bl(\Omega_3^2 - \Omega_1^2) \\ \tau y &= bl(\Omega_4^2 - \Omega_2^2) \\ \tau z &= d(\Omega_2^2 + \Omega_4^2 + \Omega_3^2 - \Omega_1^2) \end{aligned}\right\} \tag{8}$$

UAS dynamics presented in Table 2 have been utilized to get the differential equations listed above to be nonlinear and connected, which means that each differential equation is reliant on variables represented by other nonlinear equations. The analytical solutions are usually unknown. The work has been designed to solve the nonlinear model with optimization techniques, as discussed in the successive section.

B. PROBLEM FORMULATION

The primary objective of quad-copter trajectory mapping is to find a viable and optimum path towards the mark location under intricate environmental and state constraints. The coordinates of a path set point in a three-dimensional setting have been used to represent the flying space for quad-copter throughout the article [24].

$$\left\{(z,y,x)\middle| z_{\min} \le z \le z_{\max}, y_{\min} \le y \le y_{\max}, x_{\min} \le x \le x_{\max}\right\} \tag{9}$$

The flying barriers are denoted by $x_{\min}, x_{\max}, y_{\min}, y_{\max}, z_{\min}, z_{\max}$.

A simple static obstruction (x_0, y_0, z_0) is represented by a position with such a radius of the sphere (RS). Various obstacles are modeled as distributed static obstacles. A set of

$$\Re = \begin{bmatrix} Cn(\psi)\,Cn(\theta) & Cn(\psi)\,Sn(\phi)\,Sn(\theta) - Sn(\psi)\,Cn(\phi) & Sn(\phi)\,Sn(\psi) + Cn(\phi)\,Cn(\psi)\,Cn(\theta) \\ Cn(\theta)\,Sn(\psi) & Cn(\phi)\,Cn(\psi) + Sn(\phi)\,Sn(\psi)\,Sn(\theta) & Cn(\phi)\,Sn(\psi)\,Sn(\theta) - Cn(\psi)\,Sn(\phi) \\ -Sn(\theta) & Cn(\theta)\,Sn(\phi) & Cn(\phi)\,Cn(\theta) \end{bmatrix} \tag{4}$$

$$\left.\begin{aligned} \begin{bmatrix} \dot{\phi} \\ \dot{\theta} \\ \dot{\psi} \end{bmatrix} &= \begin{bmatrix} 1 & Cn(\phi)Tn(\theta) & Sn(\phi)Tn(\theta) \\ 0 & -Sn(\phi) & Cn(\phi) \\ 0 & \dfrac{Cn(\phi)}{Cn(\theta)} & \dfrac{Sn(\phi)}{Cn(\theta)} \end{bmatrix} \begin{bmatrix} p \\ r \\ q \end{bmatrix} \\ \begin{bmatrix} \dot{p} \\ \dot{q} \\ \dot{r} \end{bmatrix} &= \begin{bmatrix} \dfrac{Iy - Iz}{Ix} \\ \dfrac{Iz - Ix}{Iy} \\ \dfrac{Ix - Iy}{Iz} \end{bmatrix} \begin{bmatrix} rq \\ pr \\ pq \end{bmatrix} + \begin{bmatrix} \dfrac{\tau x + \tau wx}{Ix} \\ \dfrac{\tau y + \tau wy}{Iy} \\ \dfrac{\tau z + \tau wz}{Iz} \end{bmatrix} \\ \begin{bmatrix} \dot{u} \\ \dot{v} \\ \dot{w} \end{bmatrix} &= \begin{bmatrix} 0 & r & -q \\ -r & 0 & p \\ q & -p & 0 \end{bmatrix} \begin{bmatrix} u \\ v \\ w \end{bmatrix} + g \begin{bmatrix} -Sn(\theta) \\ Sn(\phi)Cn(\theta) \\ Cn(\phi)Cn(\theta) \end{bmatrix} + \begin{bmatrix} \dfrac{fwx}{m} \\ \dfrac{fwy}{m} \\ \dfrac{fwz - f(t)}{m} \end{bmatrix} \\ \begin{bmatrix} \dot{x} \\ \dot{y} \\ \dot{z} \end{bmatrix} &= \begin{bmatrix} Cn(\psi)Cn(\theta) & Cn(\psi)Sn(\phi)Sn(\theta) - Sn(\psi)Cn(\phi) & Sn(\phi)Sn(\psi) + Cn(\phi)Cn(\psi)Cn(\theta) \\ Cn(\theta)Sn(\psi) & Cn(\phi)Cn(\psi) + Sn(\phi)Sn(\psi)Sn(\theta) & Cn(\phi)Sn(\psi)Sn(\theta) - Cn(\psi)Sn(\phi) \\ -Sn(\theta) & Cn(\theta)Sn(\phi) & Cn(\phi)Cn(\theta) \end{bmatrix} \begin{bmatrix} u \\ v \\ w \end{bmatrix} \end{aligned}\right\} \tag{5}$$

single objects with limited space between them represents a large immovable obstacle, such as a mountain. The dynamic impediments are represented by a 6-d-o-f quad-copter model. The 'intelligent controller' should explore an alternative path that has the shortest route, the highest possible level of safety, and the least deviation from the targeted path within shorter time span.

III. MATERIALS AND METHEDOLOGY

Major advances in intelligent control, such as PID controller(s) have been used in industrial applications due to its simpler structure and design methodologies and easy implantation [25]. Systems with nonlinear dynamics affected by different physical parameters require precise accuracy in trajectory tracking. Conventional controllers must be combined with intelligent tuning strategies to balance the system's robustness and flexibility while controlling under-actuated, multi-input-multi-output UAS systems. In this context, the work has been designed for trajectory tracking based on the meta-heuristic algorithm.

A. PID CONTROL

A PID controller's performance is determined its' Proportional (k_p), Integral (k_i) & Derivative gains (k_d). The PID controller is a well-known controller that has proven to be effective and reliable in a variety of linear and nonlinear applications. The concept of PID controller enabling attitude and altitude stabilisation has been shown in Fig. 2.

A PID controller generates an error value defined as

$$e_x = x_{desired} - x_{actual} \text{ and } e_y = y_{desired} - y_{actual} \tag{10}$$

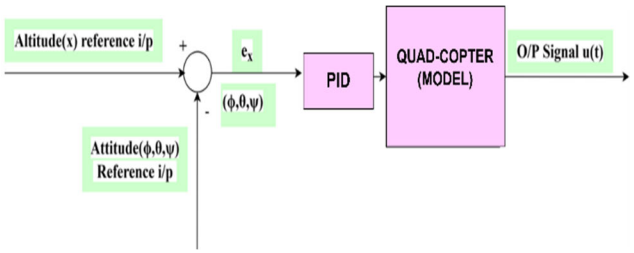

FIGURE 2. Control block diagram of nonlinear pid quad-copter's altitude and attitude control.

The controller input $u(t)$ as control parameter over time, aim to minimize the inaccuracy has been formulated as follows:

$$u(t) = k_p e(t) + k_i \int e(t) + k_d \frac{de(t)}{dt} \tag{11}$$

Consideration of the systems model can assist in fine-tuning the PID value, particularly in simulations. Minimization of error to follow the desired track assigned to UAS with different algorithms has been discussed in the coming sections. It can also be performed in real time by considering each parameter concerned.

B. PARTICLE SWARM OPTIMIZATION (PSO)

PSO is the habitually used community -based probabilistic optimization modus operandi to solve multi-parameter and Multi-variable objective functions. Animal swarms coordinate with one another to enhance their speed and the possibility of reaching the true objective in a diverse environmental course of evolution or avoiding predators. Each particle modifies it's position in the swarm to the optimum possible position based on preceding experience. Other specks modify their actions to match the swarm's instantaneous best position. It provides a better location in their new kinetics compared to the prior one. This method is repeated until the desired outcome is achieved [11].

In the search phase, each specks in the PSO algorithm exemplify a potential task solution. The velocity $(V_i^{\oplus})$ and position $(X_i^{\oplus})$ vector of the i-th particles at d-th_dimensional space are $V_i^{\oplus} = (V_{i1}, \ldots, V_{id})$ and $X_i^{\oplus} = (X_{i1}, \ldots, X_{id})$, respectively.

After the particles have been randomly initialized, the velocity $(V_i^{\oplus})$ and position $(X_i^{\oplus})$ of i-th specks are streamlined as follows:

$$V_i^{\oplus}(T+1) = w.V_i^{\oplus}(T) + c_1 r_1 (P_i - X_i^{\oplus}(T)) + c_2 r_2 (P_g - X_i^{\oplus}(T)) \tag{12}$$

$$X_i^{\oplus}(T+1) = X_i^{\oplus}(T) + V_i^{\oplus}(T+1) \tag{13}$$

where, w denotes the inertia-weight; c_1 and c_2 are constants that determine the weights of P_i and P_g; r_1 and r_2 indicate two randomly generated numbers that are distributed evenly across the range and were produced separately. [0, 1]; P_i denotes the best former stance of i-th individual, and P_g represents the generation's best prior position among all specks.

C. THE GREY WOLF OPTIMIZATION (GWO)

The Grey Wolf Optimizer [14], a unique meta-heuristic optimal approach based on simulations of grey wolf hunting behaviour and social leadership in nature, was proffered by Mirjalili et al. in 2014. Similar to anyother meta-heuristic, initiates by producing a number of aarbitary entrant solutions.

$$\left.\begin{aligned} m\left\{\begin{bmatrix}1&0&0\\0&1&0\\0&0&1\end{bmatrix}\begin{bmatrix}\dot{u}\\\dot{v}\\\dot{w}\end{bmatrix}+\begin{bmatrix}0&0&q\\0&0&-p\\0&p&0\end{bmatrix}\begin{bmatrix}u\\v\\w\end{bmatrix}+\begin{bmatrix}-ru\\ru\\-qu\end{bmatrix}\right\} &= \begin{bmatrix}-mg(Sn(\theta))+fwx\\mg(Cn(\theta)Sn(\phi))+fwy\\mg(Cn(\theta)Cn(\phi))+fwz-b(\Omega_1^2+\Omega_2^2+\Omega_3^2+\Omega_4^2)\end{bmatrix}\\ \begin{bmatrix}bl(\Omega_3^2-\Omega_1^2)\\bl(\Omega_4^2-\Omega_2^2)\\d(\Omega_2^2+\Omega_4^2+\Omega_3^2-\Omega_1^2)\end{bmatrix}+\begin{bmatrix}\tau_{wx}\\\tau_{wy}\\\tau_{wz}\end{bmatrix} &= \begin{bmatrix}\dot{p}\\\dot{q}\\\dot{r}\end{bmatrix}\begin{bmatrix}Ix\\Iy\\Iz\end{bmatrix}+\begin{bmatrix}-qrIy\\prIx\\-pqIx\end{bmatrix}+\begin{bmatrix}qrIz\\-prIz\\pqIy\end{bmatrix}\end{aligned}\right\} \tag{7}$$

TABLE 2. Parameter's used for quad-copter dynamics.

Parameters	Description	Units
$[x\ y\ z]$	Linear_ Position-Vector	m
$[\phi\ \theta\ \psi]$	Angular_ Position-Vector	rad/s
$[u\ v\ w]$	Linear_Velocity_Vector	m/s
$[p\ q\ r]$	Angular_Velocity_Vector	rad/s
$[I_x I_y I_z]$	Momentum-of-Inertia-Vector	$kg{\cdot}m^2$
f_t	Total_thrust generated-by-rotors	N
$[\tau_x\ \tau_y\ \tau_z]$	Control_Torques	$N{\cdot}m$
$[f_{wx}\ f_{wy}\ f_{wz}]$	Wind _Forcev_Vector	$\mathcal{N}$
$[\tau_{wx}\ \tau_{wy}\ \tau_{wz}]$	Wind_Torque_Vector	$N{\cdot}m$
g	Gravitational_Force	m/s^2
m	Total_Mass	kg
$[\Omega_1\Omega_2\Omega_3\Omega_4]$	Rotors_SpeedsVector	rad/s
b	Thrust co-efficient	$N{\bullet}s^2$
l	Motor-to-Center-Length	m
d	Drag_Co-efficient	$N{\cdot}m{\cdot}s^2$

$S_n() \equiv Sin(); C_n() \equiv Cos(); T_n() \equiv Tan()$

Encircling the Prey: The finest of first three wolves are regarded as alpha ($\alpha^{\oplus}$), beta ($\beta^{\oplus}$), and delta ($\delta^{\oplus}$). Throughout each iteration they direct additional wolves to probable spheres of the solution stretch. The remaining of the grey wolves are known as omega ($\omega^{\oplus}$), who constantly update their places surrounding (12).

$$\overrightarrow{D^{\oplus}} = \left|\overrightarrow{C^{\oplus}} \cdot \overrightarrow{X^{\oplus}_{p\oplus}(\mathrm{T})} - \overrightarrow{X^{\oplus}(\mathrm{T})}\right| \tag{14}$$

$$\overrightarrow{X^{\oplus}(\mathrm{T}+1)} = \overrightarrow{X^{\oplus}_{p\oplus}(\mathrm{T})} - \overrightarrow{A^{\oplus}}\overrightarrow{D^{\oplus}} \tag{15}$$

where, T = current-iteration,
$\overrightarrow{D^{\oplus}}$ = Distance between the individual current position & the target position
$\overrightarrow{A^{\oplus}}$ and $\overrightarrow{C^{\oplus}}$ are coefficient-vectors.
$\overrightarrow{X^{\oplus}_{p\oplus}(\mathrm{T})}$ = Position_Vector of prey,

In addition, three primary hunting processes are optimized: hunting for prey, enclosing prey, and attacking prey.

$\overrightarrow{X^{\oplus}(\mathrm{T})}$ = Indicates the Current _Position_Vector of a grey wolf and,
$\overrightarrow{X^{\oplus}(\mathrm{T}+1)}$ = Next position of grey wolf

While hunting for the prey, $\overrightarrow{X^{\oplus}(\mathrm{T})}$ is the position of the current solution has been given as:

$$\overrightarrow{X^{\oplus}}(\mathrm{T}+1) = \frac{\overrightarrow{X_1^{\oplus}} + \overrightarrow{X_2^{\oplus}} + \overrightarrow{X_3^{\oplus}}}{3} \tag{16}$$

$$\left.\begin{aligned}
\overrightarrow{X_1^{\oplus}} &= \overrightarrow{X_1^{\oplus}(\mathrm{T}+1)} = X^{\oplus}_{\alpha\oplus}(\mathrm{T}) - \overrightarrow{A_1^{\oplus}}\overrightarrow{D^{\oplus}_{\alpha\oplus}} \\
\overrightarrow{X_2^{\oplus}} &= \overrightarrow{X_2^{\oplus}(\mathrm{T}+1)} = X^{\oplus}_{\beta\oplus}(\mathrm{T}) - \overrightarrow{A_2^{\oplus}}\overrightarrow{D^{\oplus}_{\beta\oplus}} \\
\overrightarrow{X_3^{\oplus}} &= \overrightarrow{X_3^{\oplus}(\mathrm{T}+1)} = X^{\oplus}_{\delta\oplus}(\mathrm{T}) - \overrightarrow{A_3^{\oplus}}\overrightarrow{D^{\oplus}_{\delta\oplus}}
\end{aligned}\right\} \tag{17}$$

where $X^{\oplus}_{\alpha\oplus}(\mathrm{T})$ .... position of $(\alpha^{\oplus})$ alpha,
$X^{\oplus}_{\beta\oplus}(\mathrm{T})$ .... position of $(\beta^{\oplus})$ beta,
$X^{\oplus}_{\delta\oplus}(\mathrm{T})$ .... position of $(\delta^{\oplus})$ delta and,
$\overrightarrow{C_1^{\oplus}}$, $\overrightarrow{C_2^{\oplus}}$, $\overrightarrow{C_3^{\oplus}}$ are random vectors.

$$\left.\begin{aligned}
D^{\oplus}_{\alpha\oplus} &= \left|\overrightarrow{C_1^{\oplus}} \cdot \overrightarrow{X^{\oplus}_{\alpha\oplus}(\mathrm{T})} - \overrightarrow{X^{\oplus}(\mathrm{T}+1)}\right| \\
D^{\oplus}_{\beta\oplus} &= \left|\overrightarrow{C_2^{\oplus}} \cdot \overrightarrow{X^{\oplus}_{\beta\oplus}(\mathrm{T})} - \overrightarrow{X^{\oplus}(\mathrm{T}+1)}\right| \\
D^{\oplus}_{\delta\oplus} &= \left|\overrightarrow{C_3^{\oplus}} \cdot \overrightarrow{X^{\oplus}_{\delta\oplus}(\mathrm{T})} - \overrightarrow{X^{\oplus}(\mathrm{T}+1)}\right|
\end{aligned}\right\} \tag{18}$$

The vector's $\overrightarrow{A^{\oplus}}$ and $\overrightarrow{C^{\oplus}}$ are calculated as follows,

$$\overrightarrow{A^{\oplus}} = 2 \cdot \overrightarrow{a^*} \cdot \overrightarrow{rand_1} - \overrightarrow{a^*} \tag{19}$$

$$\overrightarrow{C^{\oplus}} = 2 \cdot \overrightarrow{rand_2} \tag{20}$$

Here $\overrightarrow{a}$ decreases linearly from 2 to 0.
Now,

$$\overrightarrow{a^*} = \left[2 - \frac{2T}{T_{\max}}\right] \tag{21}$$

Here, $\overrightarrow{a^*}$ is convergence factor and $T_{\max}$ is maximum no. of iteration.

D. DIVERSIFIED GREY WOLF OPTIMIZATION (DGWOA)

The $\omega^{\oplus}$ wolves in GWO are directed to the search areas that appear to hold promise for discovering the best solution by the $\alpha^{\oplus}$, $\beta^{\oplus}$ *and* $\delta^{\oplus}$ wolves. This behavior could lead to the entry of a locally optimum solution. Another unfavorable consequence is that reducing population diversity causes GWO to be closer to the regional optimum. In this section, the diversified grey wolf optimizer (DGWOA) is proposed as a solution to these issues. As shown in the DGWOA pseudo code, one of the improvements is a new search strategy tied to the choosing and updating processes.

To use the exploration and exploitation capabilities, operators are used in all population-based search algorithms. In order to balance exploring and taking advantage of unique search of control parameter $\overrightarrow{a^*}$ is of the GWO algorithm is vital. Local exploitation is promoted by a more modest control parameter $\overrightarrow{a^*}$, but for global exploration along with local exploitation can be achieved through proper choice of the parameter for control $\overrightarrow{a^*}$.

$$\overrightarrow{a^*} = 2\left[1 - \log\left(1 + \frac{\mu T}{T_{\max}}\right)\right] \tag{22}$$

The concept of centrifugal distance change rate has been introduced to the adaptive convergence factor strategy. An individual's current centrifugal distance can be calculated from their maximum and average centrifugal distances. The distance between an individual's current location and their preceding place in a population is known as their centrifugal distance. The distribution of potential solutions is determined by the change in centrifugal distance, and the parameter $\overrightarrow{a^*}$ is adjusted to account for nonlinear attenuation and dynamic change. Once the centrifugal distance variation rate is taken into consideration, the algorithm can search both locally and globally depending on the geographic location of the solutions.

IV. IMPLEMENTATION OF THE METHEDOLODY FOR SYSTEM STABLIZATION

The NLPID controller was designed to provide a satisfactory response for the nonlinear 6-D-o-F UASs system, as well as its derivative and integral:

$$\left.\begin{aligned} &\Lambda_{NP} = F_1(e) + F_2(\dot{e}) + F_3\left(\int e dt\right) \\ &F_j(\beta) = K_j(\beta)\,|\beta|^{x_j}\, sign(\beta) \\ &K_j(\beta) = K_{j1} + \frac{K_{j2}}{1 + \exp\left(\mu_j \beta^2\right)}, j = 1, 2, 3 \end{aligned}\right\} \tag{27}$$

where,

$$\mathbb{K}_{j1}, \mathbb{K}_{j2}, \chi_j \in \mathbb{R}$$
$$K_j(\beta) = \begin{cases} \mathbb{K}_{j1} + \dfrac{\mathbb{K}_{j2}}{2}, error \le 0 \\ \mathbb{K}_{j1}, error > 0 \end{cases}$$

The primary objective of the non-linear PID controller is to reduce the errors of $'x'$ and $'y'$ position semblance zero, as portrayed below:

$$\left.\begin{aligned} &\ddot{x}_{de} - \ddot{x}_{ac} + F_{x1}(e_x) + F_{x2}(\dot{e}_x) - F_{x3}\left(\int e_x dt\right) = 0 \\ &\ddot{y}_{de} - \ddot{y}_{ac} + F_{y1}(e_y) + F_{y2}(\dot{e}_y) - F_{y3}\left(\int e_y dt\right) = 0 \end{aligned}\right\} \tag{28}$$

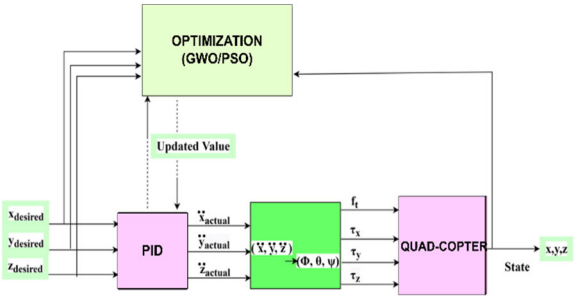

FIGURE 3. Quad-copter optimization system.

Fig. 3, shows the implementation of the optmization technique integrated with the nonlinear 6-D-o-F UAS system. In this study, system results have been compared with the desired input as a reference. The algorithm's input data, which is updated after every iteration, is referred to as the resultant error. The system's control approach has been designed to mitigate ITAE (Integral Time Absolute Error).

The objective function of a system has been given as:

$$f = \int t\,|e(t)|\,\partial t \tag{29}$$

$$fit = \begin{cases} \dfrac{1}{(1+f)}, & if\ f \ge 0 \\ 1 + |f|, & if\ f < 0 \end{cases} \tag{30}$$

where, fit = fitness function value, and f = objective function value.

Corresponding control signal of x and y of NLPID model given as:

$$\begin{aligned} U_x &= \ddot{x}_{desired} + F_x(e_x) + F_x(\dot{e}_x) + F_x(\ddot{e}_x) \\ U_y &= \ddot{y}_{desired} + F_y(e_y) + F_y(\dot{e}_y) + F_y(\ddot{e}_y) \end{aligned} \tag{31}$$

Let, $'U_x'$ and $'U_y'$ be the implicit control signals for $'x'$ and $'y'$ respectively, which proffered as (10)and (31). Where, $(F_{xj}, F_{yj}), j = 1, 2, 3$ being gain for NLPID controller, described in (27).

Lemma 1: For any uncertain nonlinear system and a controlled variable $\xi_j(t)$ to converge at a desired reference value $X_p \in \mathbb{R}$ for all the initial states $(\xi_1(0), \xi_2(0)) \in \mathbb{R}$; Stability of the given system is achieved provided the boundary condition that nonlinear function contains uncertainty necessarily.

In this context, the current position (X^*), is the controlled variable and the current position of the prey or updated position (X_p), is the desired reference value. For any uncertain nonlinear system, where the PID controller is defined for the

Algorithm 1 PSEUDOCODE 1 DGWO Algorithm

Step1: Set the population of wolves the $\overrightarrow{X_1^{\oplus}}$ (j= 1,2 …N), $T_{\max}$ is the maximum number of iterations, the parameters $\overrightarrow{a^*}$, $\overrightarrow{A^{\oplus}}$ *and* $\overrightarrow{C^{\oplus}}$, the position of the $X_{\alpha^{\oplus}}^{\oplus}$, $X_{\beta^{\oplus}}^{\oplus}$ *and* $X_{\delta^{\oplus}}^{\oplus}$ wolf. Initialize the distance matrix of each individual grey wolf to the $X_{\alpha^{\oplus}}^{\oplus}$, $X_{\beta^{\oplus}}^{\oplus}$ *and* $X_{\delta^{\oplus}}^{\oplus}$ wolf.

Step2: For all $\overrightarrow{X_1^{\oplus}}$ do

Evaluate the fitness value of each individual grey wolf by $F(X_j)$

Finish to obtain the most prominent three wolves as $X_{\alpha^{\oplus}}^{\oplus}$, $X_{\beta^{\oplus}}^{\oplus}$ *and* $X_{\delta^{\oplus}}^{\oplus}$

Step3: While ($T < T_{\max}$)

Evaluate the rate at which the centrifugal distance changes. $\mu_{\alpha^{\oplus}}$, $\mu_{\beta^{\oplus}}$, *and* $\mu_{\delta^{\oplus}}$ by Eq.(23) Eq.(24) Eq.(25)

Update $\overrightarrow{a^*}$, $\overrightarrow{A^{\oplus}}$ *and* $\overrightarrow{C^{\oplus}}$

Evaluate the difference between each individual wolf, and the $X_{\alpha^{\oplus}}^{\oplus}$, $X_{\beta^{\oplus}}^{\oplus}$ *and* $X_{\delta^{\oplus}}^{\oplus}$ wolf by Eq.(16)

Evaluate adaptive weighting factor W_{Π}^{*} can be created based on each individual's actual rate at which the centrifugal distance changes with regard to $\alpha^{\oplus}$, $\beta^{\oplus}$, and $\delta^{\oplus}$ by Eq.(25) Eq.(26)

$$Dist_{mean} = \frac{\sum_{j=1}^{N} \sqrt{\sum_{d'=1}^{d} \left(X_j^{d'} - X_{\Omega}^{d'}\right)^2}}{N}, \ \left(\Omega = \alpha^{\oplus}, \beta^{\oplus}, \delta^{\oplus}\right) \tag{23}$$

$$Dist_{\max.} = \max_{j=1,2,..N} \left(\sqrt{\sum_{d'=1}^{d} \left(X_j^{d'} - X_{\Omega}^{d'}\right)^2} \right), \ \left(\Omega = \alpha^{\oplus}, \beta^{\oplus}, \delta^{\oplus}\right) \tag{24}$$

$$\left.\begin{aligned} \mu_{\alpha^{\oplus}} &= \frac{Dist_{\alpha^{\oplus}\max.} - Dist_{\alpha^{\oplus}mean}}{Dist_{\alpha^{\oplus}\max.}} \\ \mu_{\beta^{\oplus}} &= \frac{Dist_{\beta^{\oplus}\max.} - Dist_{\beta^{\oplus}mean}}{Dist_{\beta^{\oplus}\max.}} \\ \mu_{\delta^{\oplus}} &= \frac{Dist_{\delta^{\oplus}\max.} - Dist_{\delta^{\oplus}mean}}{Dist_{\delta^{\oplus}\max.}} \end{aligned}\right\} \tag{25}$$

$$W_{\Pi}^{*} = \frac{\mu_{\Omega}}{\mu_{\alpha^{\oplus}} + \mu_{\beta^{\oplus}} + \mu_{\delta^{\oplus}}}, (\Pi = 1, 2, 3) \tag{26}$$

with respect to $\alpha^{\oplus}$, $\beta^{\oplus}$ *and* $\delta^{\oplus}$

Update $\overrightarrow{X_1^{\oplus}}$ by Eq. (26) For all $\overrightarrow{X_1^{\oplus}}$ Evaluate each grey wolf's fitness level separately by $f\left(X_j(T)\right)$

End for

Get the best three best wolves as $X_{\alpha^{\oplus}}^{\oplus}$, $X_{\beta^{\oplus}}^{\oplus}$ *and* $X_{\delta^{\oplus}}^{\oplus}$;

Update $X_{\alpha^{\oplus}}^{\oplus}$, $X_{\beta^{\oplus}}^{\oplus}$ *and* $X_{\delta^{\oplus}}^{\oplus}$

$T = \mathrm{T} + 1$;

End while Return $X_{\alpha^{\oplus}}^{\oplus}$

End.

values of (K_P, K_I, K_D), the closed loop system will satisfy $\lim_{t\to\infty} X(t) = X_p$ for any nonlinear function, any set point $X_p \in \mathbb{R}^n$ and initial state $X(0) \in \mathbb{R}^n$ [26].

Theorem_1: The certain NLPID controller as discussed in (10), (27)-(31) for the (35), is Hurwitz stable for a closed loop for $\mathbb{K}_1(e_1) \in \left[\mathbb{K}_{11}, \mathbb{K}_{11} + \frac{\mathbb{K}_{12}}{2}\right]$, $\mathbb{K}_3(e_0) \in \left[\mathbb{K}_{31}, \mathbb{K}_{31} + \frac{\mathbb{K}_{32}}{2}\right]$ and, $\mathbb{K}_2(e_2) \in \left[\mathbb{K}_{21}, \mathbb{K}_{21} + \frac{\mathbb{K}_{22}}{2}\right]$, provided that all the state variables for the quadcopter are the observable state, and, the tuned value of α for the six controller of the UASs be around 1.

Proof: Suppose consider the following nonlinear model of a given uncertain second-order nonlinear system, represented by 2nd order Brunovsky form as:

$$\left.\begin{aligned} \dot{\xi}_j &= \xi_2 \\ \dot{\xi}_2 &= \iota_u + h\gamma_{\xi} \end{aligned}\right\} \tag{32}$$

where,

$$\begin{aligned} \xi_1 &= \{x, y, z, \phi, \theta, \psi\} \in \mathbb{R} \\ \xi_2 &= \{u, v, w, p, q, r\} \in \mathbb{R} \\ \gamma_{\xi} &= \left\{U_x, U_y, -U_z, U_{\phi}, U_{\theta}, U_{\psi}\right\} \in \mathbb{R} \\ h &\in \mathbb{R} \end{aligned}$$

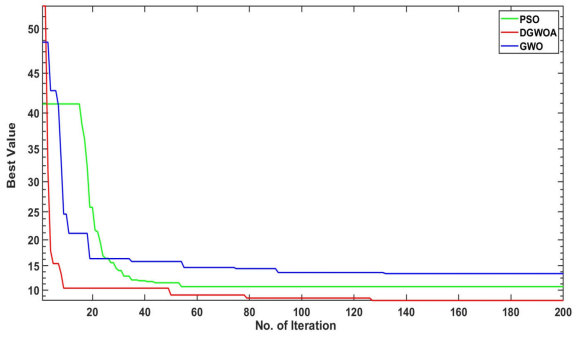

FIGURE 4. Convergence curve of best fitness value with respect of increase of iteration times.

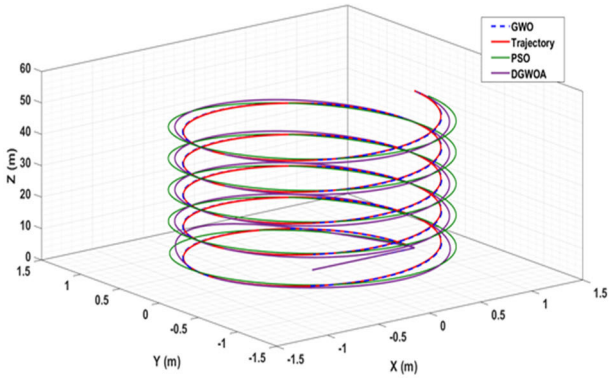

FIGURE 5. Helical tracking.

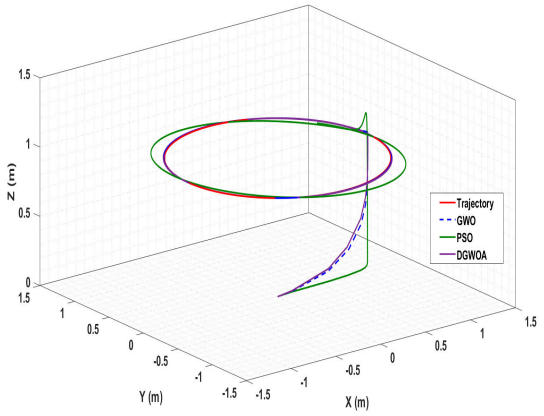

FIGURE 6. Circular tracking.

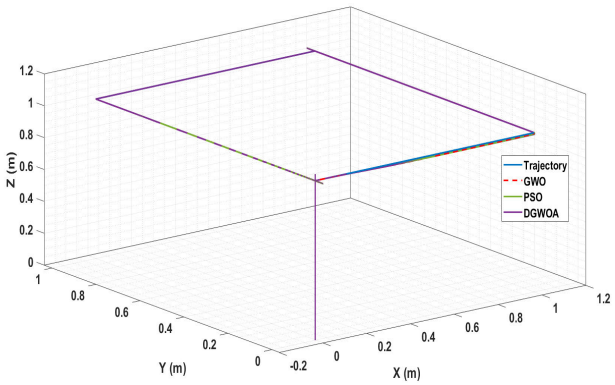

FIGURE 7. Square tracking.

Here, in (32), 'ι_u' is an anonymous function, which has been neglected, as in proffered nonlinear PID controller, belonging to a passive controller, which is unable to estimate the unknown function by itself. The (32) then can be rewritten as:

$$\left.\begin{aligned}\dot{\xi}_j &= \xi_2 \\ \dot{\xi}_2 &= h\gamma_\xi\end{aligned}\right\} \tag{33}$$

The suggested closed-loop system's error dynamics are expressed as:

$$\left.\begin{aligned}e_1 &= \xi_{1de} - \xi_{1ac} \\ e_2 &= \xi_{2de} - \xi_{1ac} \\ e_0 &= \int e_1 dt\end{aligned}\right\} \tag{34}$$

Using the derivatives of (34) while also being aware of $\dot{\xi}_{1de} = \xi_{2de}$ and $\dot{\xi}_{2de} = 0$ producing results,

$$\left.\begin{aligned}\dot{e}_0 &= e_1 \\ \dot{e}_1 &= e_2 \\ \dot{e}_2 &= -h\gamma_\xi\end{aligned}\right\} \tag{35}$$

Substituting, the above (35) into (27), expressing in matrix form,

$$\begin{bmatrix}\dot{e}_0 \\ \dot{e}_1 \\ \dot{e}_2\end{bmatrix} = A_c \begin{bmatrix}e_0 \\ e_1 \\ e_2\end{bmatrix} \tag{36}$$

where,

$$A_c = \begin{bmatrix}0 & 1 & 0 \\ 0 & 0 & 1 \\ -h\mathbb{K}_3(e_0) & -h\mathbb{K}_1(e_1) & -h\mathbb{K}_2(e_2)\end{bmatrix}$$

With, $|\lambda\mathbb{I} - A_c| = 0$, yields the characteristics equation for A_c as,

$$\lambda^3 + h\mathbb{K}2(e_2)\lambda^2 + h\mathbb{K}_1(e_1)\lambda + h\mathbb{K}_3(e_0) = 0 \tag{37}$$

The Hurwitz-Matrix ($\mathbb{H}$) for characteristics equation is denoted as,

$$\mathbb{H} = \begin{bmatrix}h\mathbb{K}_2(e_2) & h\mathbb{K}_3(e_0) & 0 \\ 1 & h\mathbb{K}_1(e_1) & 0 \\ 0 & h\mathbb{K}_2(e_2) & h\mathbb{K}_3(e_0)\end{bmatrix}$$

The system (37) to be stable according to ($\mathbb{H}$) be:

$$\begin{aligned}\Delta_1 &= h\mathbb{K}_2(e_2) > 0 \\ \Delta_2 &= h^2\mathbb{K}_1(e_1)\mathbb{K}_2(e_2) - h\mathbb{K}_3(e_0) > 0 \\ \Delta_3 &= h^3\mathbb{K}_1(e_1)\mathbb{K}_2(e_2)\mathbb{K}_3(e_0) - h^2\mathbb{K}_3^2(e_0) > 0 \\ \Delta 3 &= h\mathbb{K}_3(e_0)\Delta_2 > 0\end{aligned}$$

As stated earlier, $K_j(\beta)$ is a sector bounded in the range $\left[\mathbb{K}_{j1}, \mathbb{K}_{j1} + \frac{\mathbb{K}_{j2}}{2}\right]$ and consistently in the positive, considering

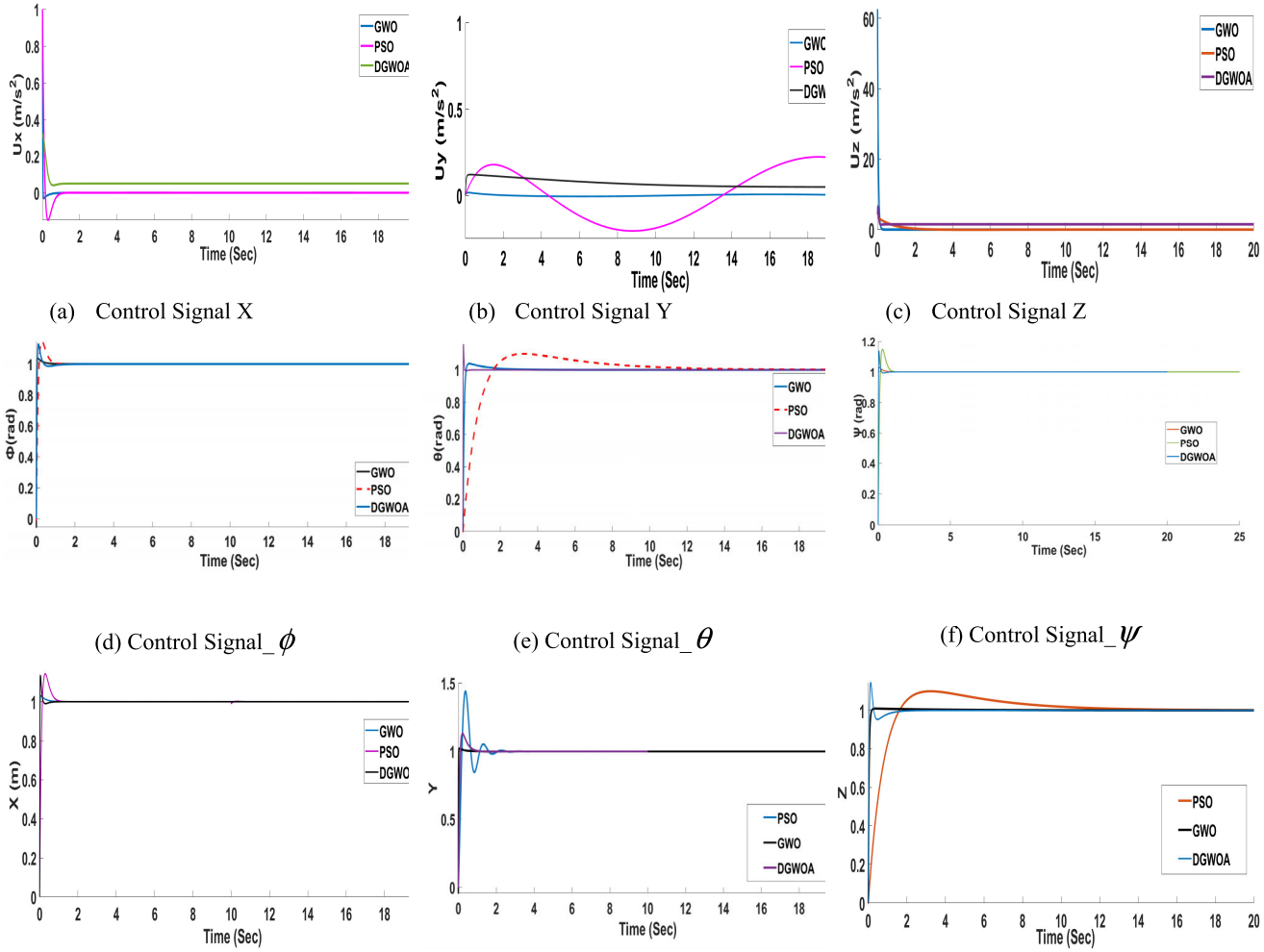

(a) Control Signal X (b) Control Signal Y (c) Control Signal Z

(d) Control Signal_ ϕ (e) Control Signal_ θ (f) Control Signal_ ψ

(g) Time Response Signal x (h) Time Response Signal y (i) Time Response Signal z

FIGURE 8. Position response of the quad-copter.

a region for any two of $\{\mathbb{K}_1(e_1), \mathbb{K}_2(e_2), \mathbb{K}_3(e_0)\}$ eventually leading to the region of third, which ensures that the closed-loop system is enduring & stable in terms of the Hurwitz-Stability theorem.

V. SIMULATION RESULT AND DISCUSSION

This section discusses the different optimization approaches that have been applied in order to deal with this section discusses the different optimization approaches that have been applied in order to deal with nonlinear behavior of the system. To visualize the effects of the individual algorithm in more clear manner, the convergence curve of fitness values for various algorithm adopted in the process of path planning are depicted in Fig. 4. Various parameters for the algorithms are defined in Appendix B. The convergence of the GWO and PSO algorithms occurs at iterations 15 and 30, respectively. In comparison to the proposed DGWOA, PSO and GWO require a longer duration to reach convergence. Analyzing convergence precision, the GWO and PSO algorithms have challenges in determining the optimal flying route. PSO's mean and standard deviation are 4.6513 and 0.0733, respectively, with a computation time of 1.6483 seconds. While DGWOA performs with 2.7379 and 0.0796, GWO has a standard deviation and mean of 3.8135 and 0.081, respectively, with a computing time of 0.1726 seconds. DGWOA requires a minimum of 0.1456 seconds, which is shorter than GWO's.

The outturn responses of three different simulation cases with track-route obtained by MATLAB/Simulink has been discussed here on. The trajectory cases studied [4], [27], [28] were chosen to illustrate the significant problems that the quad-copter system may encounter when attempting to achieve the required tracking. Nonlinear 6-D-o-F quad-copter's objective function has endured many case studies as a result of optimization technique.

CASE 1: Implementation of reference trajectories for halical path has been performed with reference trajectrory $u(t)$, $Cos(0.1\pi t)$ *and*, $Sin(0.1\pi t)$ for input x, y and z respectivly for the duration of initial time $t_0 = 0$ to final time t_f.

TABLE 3. Position and attitude response for quad-copter.

Methodology	Parameters	Rise Time	Settling Time	Max. Peak Overshoot	Max	Min
PSO	ϕ	1.921mSec	2.507mSec	0.5%	1.001	0
	θ	1.05914mSe	0.95Sec	14.368%	1.147	-9.487e-03
	ψ	1.117Sec	15.6125 Sec	10.556%	1.1	-1.036e-0.3
	x	1.988mSec	0.12 Sec	0.502%	-	-
	y	143.25mSec	2.3 Sec	44.203%	1.44	-1.01 e-0.2
	z	1.921mSec	8.8 Sec	0.556%	11	-1.043 e-0.3
GWO	ϕ	2.492m Sec	3.304mSec	0.386%	1.001	0
	θ	19.25mSec	0.625Sec	3.804%	1.039	-5.394e-02
	ψ	102.03m Sec	2.25Sec	3.646%	1.039	-2.695e-05
	x	3.678mSec	0.755 Sec	0.447%	-	-
	y	10.566mSec	0.755 Sec	2.66%	1.022	-4.058 e-0.3
	z	86.726mSec	1.206 Sec	0.505%	1	1
DGWOA	ϕ	3.2292m Sec	0.311Sec	1.3068%	1.128	0
	θ	7.543m Sec	1.71Sec	1.46%	1.159	0
	ψ	16.637m Sec	0.38 Sec	1.4368%	1.38	0
	x	3.553m Sec	1.53 Sec	1.3068%	1.136	0
	y	47.867m Sec	1.21 Sec	1.3068%	1.132	0
	z	48.294m Sec	1.688 Sec	1.4368%	1.146	0
Reference [4]	x	1.15 Sec	4.657 Sec	0.505%		
	y	1.572 Sec	3.023 Sec	0.195%		
	z	0.677 Sec	1.283 Sec	0.505%		

TABLE 4. ITAE performance index.

Parameters	Methodology	ITAE	Methodology	ITAE	Methodology	ITAE	Methodology	ITAE
x	GWO	0.0136	PSO	0.0321	DGWOA	0.0263	[4]	14.285931
y		270		301		263		7.498694
z		8.699		8.689		8.06		0.059225

For the duration of the simulation, the proposed control strategy algorithm performed better compared to GWO and PSO, as later one continues to follow the reference trajectory with a constant offset, as in Fig. 5.

CASE 2: Reference input for a 6-D-o-F quad-copter has been provided along with an iterative and incremental approach, circular track is shown in Fig. 6. The current states of x, y and z endow with $0.2t$, $Cos(0.1\pi t)$ *and*, $Sin(0.1\pi t)$ respectively for the time period $t_0 = 0$ to final time t_f. The result shows that the proposed algorithm has less error as the quad-copter follows the specified path with slightest deviation.

CASE 3: Furthermore, since the situations mentioned above are based on rotation, and this case contains a 90-degree phase shift, square track has been taken into consideration. x, y and z have been implemented with $u(t-30)-u(t-70)$, $u(t-10)-u(t-50)$ *and*, $u(t)$ reference trajectories to confirm the trajectory as presented in Fig. 7.

The nonlinear 6-D-o-F quad-copter system has responded well to the change in the reference input based on an optimization technique. Figure 8 depicts the control signals for the 6-D-o-F quad-copter, illustrating the controller's performance. The position and attitude control parameters have step inputs with reference applied to them. Fig. 8 (a), (b), and (c) present the control signal for and, respectively, the energy required by the quad-copter to attain the desired position through the DGWOA, GWO, and PSO algorithms. It can be seen that the DGWOA controller produces a less fluctuating control signal than the PSO controller; also, the DGWOA controller has a quicker response than the PSO and GWO controllers, except in the z-position, where the PSO controller has faster traceability, but this is due to the large amount of control energy spent. In practice, this increase in control signal energy is undesirable because it causes actuator saturation. The output interactions ϕ, θ *and* ψ are shown in Fig. 8 (d), (e), and (f), demonstrating the

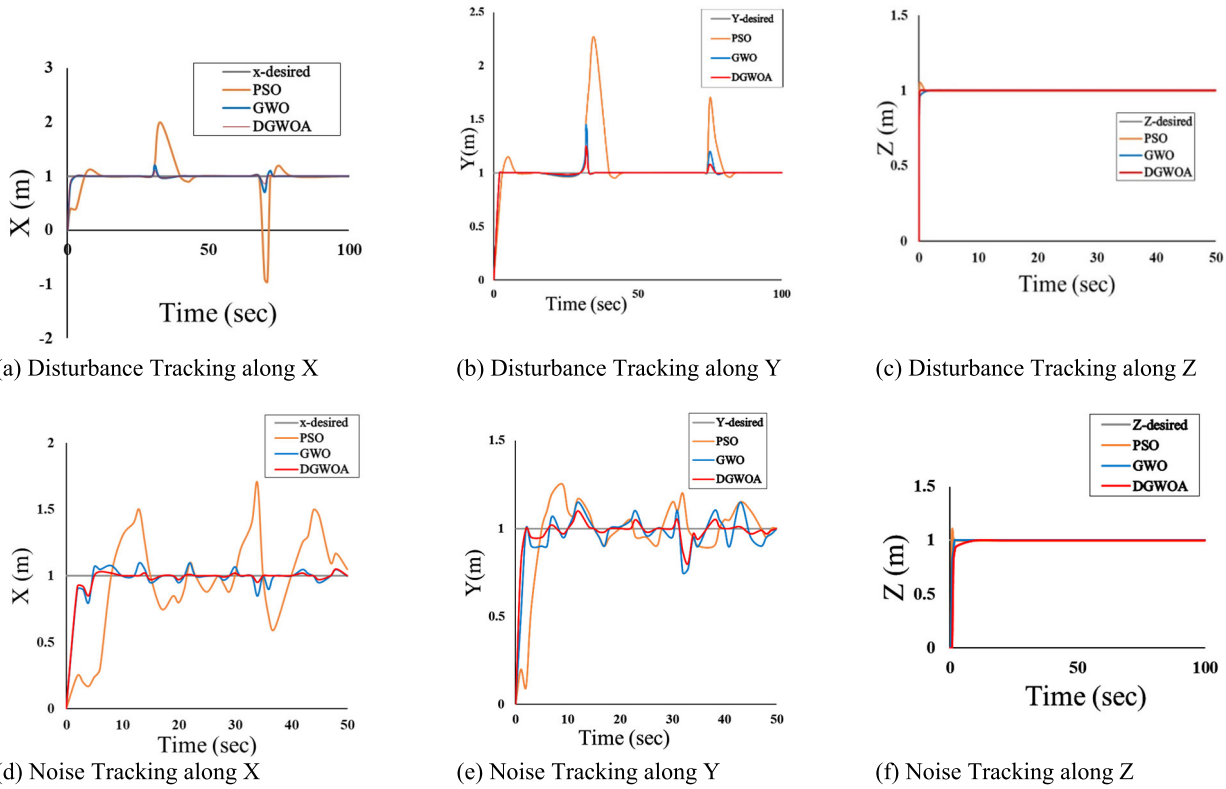

(a) Disturbance Tracking along X (b) Disturbance Tracking along Y (c) Disturbance Tracking along Z

(d) Noise Tracking along X (e) Noise Tracking along Y (f) Noise Tracking along Z

FIGURE 9. **Disturbance & noise based tracking of a quad-copter position.**

efficacy of the proposed DGWOA control algorithm over the PSO and GWO. The statistical analysis has been presented in Table 3, which indicates the position and attitude responses of the proffered algorithm. This is reflected in the control signal's energy and the sleekness of the output parameters. When the energy impulses ϕ, θ *and* ψ were compared using those controllers, the DGWOA controller showed a significant reduction when compared against the other algorithms. Table 3 shows the time domain performance (Rise Time, Settling Time, and Max. Peak Overshoot) and also displays the maximum and minimal peak values for the quad-rotor system's position and attitude. It can be observed that the DGWOA controller has a quicker response to the control signals along the y and z axes when compared with GWO and PSO. Thus, the DGWOA algorithm shows better performance in any scenario when compared to the reference, (z, y, x) has been improved with (92.87, 96.95, and 99.69) percentage.

According to the results (Fig. 5, 6, and 7), there are no trajectory deviations or direction changes when the quad coptor's trajectory integrates with the reference trajectory. In addition to accurately following the stated trajectory, the proposed DGWOA controller also performs better in terms of position response as well as disturbance tracking, steady-state error, and overshoot compared to other reference controllers.

The performance index of the designed quad-copter in terms of the ITAE is depicted in Table 4. From the table, its' clear that DGWOA has lowest value for ITAE, providing better stability to the system.

To check the robustness of the different algorithm, disturbances are introduced at the different interval of time, as shown in figure 8. We tried comparing the efficacy of the proffered controller with other controllers in the existence of endogenous rumpus as well as measurement of noise. Step references are used for the quad-copter's position along with attitude when it is countenance unity pulses wind rumpus, which are solicited to the horizontal plane of the 6-D-o-F quad-copter system. The findings indicate that the proposed controller attenuates the rumpuses in a short span of time with tiny peaks in the output retort. The other algorithm, on the other hand, responds to disruptions with a lack of efficacy as well as exorbitant over and/or undershoots with output response. From the Fig. 9 (a), (b), and (c), it's evident that proposed controller is quicker and more efficient at handling the disturbances. When compared with other optimization method at time interval 30sec and 80sec respectively, in Fig. 9 (a), and (b), DGWOA optimizes the signal faster with smaller kinks. Simultaneously, the effect of noise on system performance has been shown in Fig. 9 (d), (e), and (f). DGWOA can be seen, settling the signal faster with smaller kinks. It also validates the DGWOA's performance by detecting noise in the acquired data. All of the states are depicted in Fig. 9.

TABLE 5. List of abbreviations.

Abbreviation	Full Text
UAS	Unmanned Aerial System
PI	Proportional Integral
PID	Proportional Integral Derivative
LPID	Linear Proportional Integral Derivative
NLPID	Non- Linear Proportional Integral Derivative
PSO	Particle Swarm Optimization
APSO	Advanced Particle Swarm Optimization
ACO	Ant Colony Optimization
DE	Differential Evolution
GWO	Grey Wolf Optimizer
DoF	Degree of Freedom
ITAE	Integral of Time Absolute Error
OPI	Output Performance Index
DGWOA	Diversified Grey Wolf Optimization Algorithm
MIMO	Multi Input Multi Output
LQR	Linear Quadratic Regulator

TABLE 6. Parameters of the proposed algorithm.

PSO	GWO	DGWOA
Population=50, Iteration =200 $V_{max} = 6$ $w_{max} = 0.9$ $w_{min} = 0.1$ $C_1 = 2$ $C_2 = 2$	Population=50, Iteration =200 Dimension = 4 Lower bound = 0 Upper bound = 10	Population=50, Iteration =200 Lower bound = 0 Upper bound = 10 Dimension = 4 $\overrightarrow{a^*}$ = [0,2] Adaptive weighting factor $W^*_{\Pi(\alpha^{\oplus},\beta^{\oplus},\delta^{\oplus})}$ =0.5, 0.4, 0.1

VI. CONCLUSION

This article introduces mathematical frameworks and approaches to address the challenges of nonlinear systems, such as quad-copters for trajectory tracking. The nonlinear system can be handled by linearizing it, but the practical impact of nonlinearity can't be neglected. To improve the dynamic response as well as trajectory tracking of non-linear systems, meta-heuristic algorithms have been integrated with traditional controllers. The controller parameters have been optimized using PSO, GWO, and DGWO. Implementation of an appropriate algorithm that can handle non-linearity and the performance evaluation prospects: these algorithms have been compared based on the convergence factor. It shows the DGWO algorithm reaches its best value in 7 iterations. System responses undergo different case studies with different disturbances and noise signals. Not just graphical responses, but statistics also support the performance of the DGWO algorithm, which is better than the PSO and GWO. Some limitations of the proposed algorithm are that it is a challenging task to deal with a nonlinear model. To prevent it from becoming stuck in local minima, more attention must be given during algorithm design. Future work will involve changing the design of the path planning (Flight) controller in consideration of the simulation responses.

APPENDIX

Appendixes 'A', consists of list of the abbreviations used in this paper. Appendixes 'B', consists of list of the parameters used for the proffered Algorithm for this paper.

APPENDIX A

See Table 5.

APPENDIX B

See Table 6.

REFERENCES

[1] A. L. Salih, M. Moghavvemi, H. A. F. Mohamed, and K. S. Gaeid, "Modelling and PID controller design for a quadrotor unmanned air vehicle," in *Proc. IEEE Int. Conf. Autom., Quality Test., Robot. (AQTR)*, May 2010, pp. 1–5.

[2] M. H. Tanveer, D. Hazry, S. F. Ahmed, M. K. Joyo, and F. A. Warsi. (2013). *Design of Overall Stabilized Controller for Quad-Rotor*. [Online]. Available: https://www.researchgate.net/publication/256081749

[3] M. Baumann, S. Léonard, E. A. Croft, and J. J. Little, "Path planning for improved visibility using a probabilistic road map," *IEEE Trans. Robot.*, vol. 26, no. 1, pp. 195–200, Feb. 2010, doi: 10.1109/TRO.2009.2035745.

[4] A. A. Najm and I. K. Ibraheem, "Nonlinear PID controller design for a 6-DOF UAV quadrotor system," *Eng. Sci. Technol., Int. J.*, vol. 22, no. 4, pp. 1087–1097, Aug. 2019, doi: 10.1016/J.JESTCH.2019.02.005.

[5] J. Xu, Y. Zeng, and R. Zhang, "UAV-enabled wireless power transfer: Trajectory design and energy optimization," *IEEE Trans. Wireless Commun.*, vol. 17, no. 8, pp. 5092–5106, Aug. 2018.

[6] C. Huang, "A novel three-dimensional path planning method for fixed-wing UAV using improved particle swarm optimization algorithm," *Int. J. Aerosp. Eng.*, vol. 2021, Jul. 2021, Art. no. 7667173, doi: 10.1155/2021/7667173.
[7] B. Tong, L. Chen, and H. Duan, "A path planning method for UAVs based on multi-objective pigeon-inspired optimisation and differential evolution," *Int. J. Bio-Inspired Comput.*, vol. 17, no. 2, p. 105, 2021, doi: 10.1504/IJBIC.2021.114079.
[8] Y. Kim, D.-W. Gu, and I. Postlethwaite, "Real-time optimal mission scheduling and flight path selection," *IEEE Trans. Autom. Control*, vol. 52, no. 6, pp. 1119–1123, Jun. 2007, doi: 10.1109/TAC.2007.899048.
[9] J. Tang, X. Chen, X. Zhu, and F. Zhu, "Dynamic reallocation model of multiple unmanned aerial vehicle tasks in emergent adjustment scenarios," *IEEE Trans. Aerosp. Electron. Syst.*, vol. 59, no. 2, pp. 1139–1155, Apr. 2023, doi: 10.1109/TAES.2022.3195478.
[10] P. K. Mohanty and H. S. Dewang, "A smart path planner for wheeled mobile robots using adaptive particle swarm optimization," *J. Brazilian Soc. Mech. Sci. Eng.*, vol. 43, no. 2, p. 101, Feb. 2021, doi: 10.1007/s40430-021-02827-7.
[11] A. M. Hasan and S. M. Raafat, "Optimized formation control of multi-agent system using PSO algorithm," *Indonesian J. Electr. Eng. Comput. Sci.*, vol. 20, no. 3, p. 1591, Dec. 2020, doi: 10.11591/ijeecs.v20.i3.pp1591-1600.
[12] M. Abdulakareem and F. Raheem, "Development of path planning algorithm using probabilistic roadmap based on ant colony optimization," *Eng. Technol. J.*, vol. 38, no. 3A, pp. 343–351, Mar. 2020, doi: 10.30684/etj.v38i3A.389.
[13] J. Tang, G. Liu, and Q. Pan, "A review on representative swarm intelligence algorithms for solving optimization problems: Applications and trends," *IEEE/CAA J. Autom. Sinica*, vol. 8, no. 10, pp. 1627–1643, Oct. 2021, doi: 10.1109/JAS.2021.1004129.
[14] S. Mirjalili, S. Mohammad, and A. Lewis, "Grey wolf optimizer," *Adv. Eng. Softw.*, vol. 69, pp. 46–61, Mar. 2014.
[15] C. Zheng, Y. Su, and P. Mercorelli, "A simple nonlinear PD control for faster and high-precision positioning of servomechanisms with actuator saturation," *Mech. Syst. Signal Process.*, vol. 121, pp. 215–226, Apr. 2019, doi: 10.1016/j.ymssp.2018.11.017.
[16] X. Yu and J. Jiang, "A survey of fault-tolerant controllers based on safety-related issues," *Annu. Rev. Control*, vol. 39, no. 1, pp. 46–57, Oct. 2015, doi: 10.1016/j.arcontrol.2015.03.004.
[17] C. Schumacher and S. Singh, "Nonlinear control of multiple UAVS in close-coupled formation flight," in *Proc. AIAA Guid., Navigat., Control Conf. Exhib.*, Oct. 2000, p. 4373, doi: 10.2514/6.2000-4373.
[18] H. Khan and M. Kadri, "Position control of quadrotor by embedded PID control with hardware in loop simulation," in *Proc. 17th IEEE Int. Multi Topic Conf.*, Oct. 2014, pp. 395–400, doi: 10.1109/INMIC.2014.7097372.
[19] J. Zhang, Z. Ren, C. Deng, and B. Wen, "Adaptive fuzzy global sliding mode control for trajectory tracking of quadrotor UAVs," *Nonlinear Dyn.*, vol. 97, no. 1, pp. 609–627, Jul. 2019, doi: 10.1007/s11071-019-05002-9.
[20] N. Hadi and A. Ramz, "Tuning of PID controllers for quadcopter system using hybrid memory based gravitational search algorithm—Particle swarm optimization," *Int. J. Comput. Appl.*, vol. 172, no. 4, pp. 9–18, Aug. 2017.
[21] J.-J. Xiong and E.-H. Zheng, "Position and attitude tracking control for a quadrotor UAV," *ISA Trans.*, vol. 53, no. 3, pp. 725–731, May 2014, doi: 10.1016/j.isatra.2014.01.004.
[22] P. Lyu, J. Lai, J. Liu, H. H. T. Liu, and Q. Zhang, "A thrust model aided fault diagnosis method for the altitude estimation of a quadrotor," *IEEE Trans. Aerosp. Electron. Syst.*, vol. 54, no. 2, pp. 1008–1019, Apr. 2018, doi: 10.1109/TAES.2017.2773262.
[23] R. Sanz, P. García, Q.-C. Zhong, and P. Albertos, "Predictor-based control of a class of time-delay systems and its application to quadrotors," *IEEE Trans. Ind. Electron.*, vol. 64, no. 1, pp. 459–469, Jan. 2017, doi: 10.1109/TIE.2016.2609378.
[24] Y. V. Pehlivanoglu and A. Hacioglu, "Vibrational genetic algorithm based path planner for autonomous UAV in spatial data based environments," in *Proc. 3rd Int. Conf. Recent Adv. Space Technol.*, Jun. 2007, pp. 573–578.
[25] P. Priya and S. Kamlu, "Improved GA-PI technique for non-linear dynamic modelling of a UAV," in *Proc. Int. Conf. Connected Syst. Intell. (CSI)*, Aug. 2022, pp. 1–6, doi: 10.1109/CSI54720.2022.9924088.
[26] C. Zhao and L. Guo, "Towards a theoretical foundation of PID control for uncertain nonlinear systems," *Automatica*, vol. 142, Aug. 2022, Art. no. 110360, doi: 10.1016/j.automatica.2022.110360.
[27] W. Wu, J. Xu, C. Gong, and N. Cui, "Adaptive path following control for miniature unmanned aerial vehicle confined to three-dimensional Dubins path: From take-off to landing," *ISA Trans.*, vol. 143, pp. 156–167, Dec. 2023, doi: 10.1016/J.ISATRA.2023.09.021.
[28] H. M. Jayaweera and S. Hanoun, "A dynamic artificial potential field (D-APF) UAV path planning technique for following ground moving targets," *IEEE Access*, vol. 8, pp. 192760–192776, 2020.

PARUL PRIYA (Member, IEEE) was born in India. She is currently pursuing the Ph.D. degree in electrical and electronics engineering with the Birla Institute of Technology, Mesra, Ranchi, India. Her research interests include robust control, optimal control systems, soft computing, and intelligent control for path planning and their applications in autonomous vehicles.

SUSHMA S. KAMLU was born in India, in 1982. She received the B.E. degree in electrical from Swami Ramanand Teerth Marathwada University, Nanded, India, and the M.E. and Ph.D. degrees in electrical from the Birla Institute of Technology (BIT), Mesra, India. She is currently an Assistant Professor with the Department of Electrical and Electronic Engineering, BIT. She has 16 years of teaching experience. Her research interests include control systems, control systems and drives, optimal control theory, soft computing applications, reliability, and control.